

Numerical simulation of top-emitting organic light-emitting diodes with electron and hole blocking layers

Shu-Hsuan Chang^{*a} and Cheng-Hong Yang^b

^aDept. of Industrial Educ. and Tech., Nat'l Changhua Univ. of Education, Changhua 500, Taiwan

^bInstitute of Photonics, National Changhua University of Education, Changhua 500, Taiwan

ABSTRACT

The few reported high-contrast organic light-emitting diodes (OLEDs) all deal with bottom-emitting OLEDs and may not be readily adapted for top-emitting OLEDs (TOLEDs), which have a few technical merits over bottom-emitting devices for high-performance active-matrix OLED displays (AMOLEDs). The thin-film transistors on the back-plane of an AM substrate reduce the aperture ratio of a pixel that decreases the display brightness. A TOLED, which can provide a more flexible pixel design on an opaque AM substrate, represents a promising technique for achieving a high aperture-ratio AMOLED. In this work, the characteristics of TOLEDs with α -NPD and LiF blocking layers are numerically investigated with the APSYS simulation program. The α -NPD layer is used as an electron blocking layer, while the LiF layer is used as a hole blocking layer. The TOLED structure used in this study is based on a real device fabricated in lab by Yang *et al.* (Appl. Phys. Lett. 87, 143507, 2005). The simulation results indicate that when the TOLED device is with either α -NPD or LiF blocking layer, the luminance efficiency and radiative recombination rate at the same drive voltage can be markedly improved. The TOLED with α -NPD blocking layer has the best performance when the position of light emission is located at the anti-node of the standing wave due to micro-cavity effect. The TOLED with LiF blocking layer has improved performance because the LUMO of Alq₃ can be lowered by band bending, which leads to better carrier balance and thus increased radiative recombination rate.

Keywords: OLED, blocking layer, micro-cavity effect, numerical simulation

1. INTRODUCTION

Organic light-emitting diodes (OLEDs) have attracted much attention in recent years because of the superior characteristics such as high brightness, fast response time, wide angle, and low operating voltage.^{1,2} The few reported high-contrast OLED structures all deal with bottom-emitting OLEDs and may not be readily adapted for top-emitting OLEDs (TOLEDs), which have a few technical merits (e.g., larger aperture ratios) over bottom-emitting devices for high-performance active-matrix OLED (AMOLED) displays.³⁻⁵ Although the cost is relatively low, the passive-matrix (PM) architecture requires high peak current to provide high luminance, resulting in high power consumption along with adverse effects on the OLEDs reliability.⁶ On the other hand, the AM technique is more suitable for large size, high quality, and long lifetime application.⁷ However, the thin-film transistors (TFTs) on the back-plane of an AM substrate reduce the aperture ratio of a pixel that decreases the display brightness. On the contrary, TOLED, which can provide a more flexible pixel design on an opaque AM substrate, represents a promising technique for achieving a high aperture-ratio AMOLED.⁸ The performance of TOLED is still far from perfection due to the limited efficiency. High brightness and efficiency rely on efficient and balanced recombination.⁹ In order to enhance the OLED performance, the carriers should recombine in the emitting layer, so a thin LiF hole blocking layer (HBL), which can block the holes from drifting ahead, may be inserted between the cathode and emitting layer for this purpose.¹⁰ Lee *et al.* proposed that an α -NPD electron blocking layer (EBL) can be used in the interface between independent emitting layers to partly hinder the electron transport, and confine some electrons in the recombination zone.¹¹

In this work, we numerically investigate the optical and electronic properties of TOLED structures with electron and hole blocking layers by means of the APSYS (Advanced Physical Model of Semiconductor Devices) simulation program, which combines the physical models developed by Ruhstaller *et al.*¹², Hoffmann *et al.*¹³, and Henry *et al.*¹⁴ for simulating the electronic and optical processes, as well as the micro-cavity effect in multilayer TOLEDs.

*shc@cc.ncue.edu.tw; phone 886 4 723-2105 ext. 7262; fax 886 4 721-1097; http://shc.ncue.edu.tw/

By inserting a α -NPD electron blocking layer, the electrons can be confined in the recombination zone and hence the TOLED performance can be effectively enhanced. We investigate the optimal position of the α -NPD layer in the Alq₃, because the performance of the device depends on the position of electron blocking layer in the Alq₃, the electron injection, the recombination efficiency, and the micro-cavity effect. Moreover, by inserting a LiF hole blocking layer, the TOLED performance can be further improved, because the higher HOMO of LiF can help keep the holes in the recombination zone to increase the carrier balance. Note that the position of the recombination zone is not changed with the use of a LiF layer. Hence, the TOLED with both electron and hole blocking layers is beneficial for achieving high brightness and efficiency because the luminance and carrier balance can be improved due to micro-cavity effect.

2. PHYSICAL MODEL AND PARAMETERS

The numerical analysis was executed by the APSYS simulation program developed by Crosslight Inc. This program can be used to simulate the light-emitting diodes (LEDs), solar cell, organic light-emitting diodes (OLEDs), resonant-cavity light-emitting diodes (RC-LEDs), and high-electron-mobility transistors (HEMTs) of different material systems.¹⁵ The OLED characteristics are simulated by solving the Poisson's equation, the current continuity equations for electrons and holes. Unlike traditional LEDs, the charge transport in OLEDs is activated by the electric field in a hopping-like model.^{12, 16-17} In the meantime, the organic semiconductor emits light via Frenkel exciton recombination and the mechanism of light absorption and emission is different from the conventional semiconductor theories based on free-carrier/many-body band-to-band transitions.¹⁸ The optical spectrum theory for organic material is generally rather complicated due to the complexity in molecular structure. In this study, simplified exciton model based on the Holstein model is used to obtain the emission and absorption spectra.¹⁹ The Holstein model assumes that a one-dimensional molecular chain links the intra-molecular, and inter-molecular electronic and vibronic interactions exist between a limited numbers of nearest neighbors. The optical spectrum model based on exciton-phonon interaction within an organic crystal is used to calculate the OLED emission spectra. Moreover, for TOLED devices, the micro-cavity effect needs to be carefully considered because both anode and cathode electrodes are made by metals. Coupling of spontaneous emission with micro-cavity modes is presented based on Fabry-Perot devices in Green's function method.¹⁴

3. SIMULATION RESULTS AND DISCUSSION

The typical TOLED structure²⁰ and the TOLED with a α -NPD electron blocking layer are shown in Fig. 1. The m-MTDATA (4,4',4''-tris(3-methylphenylphenylamino)triphenylamine) layer is the hole injection layer (HIL) of the TOLED structure, the α -NPD (α -naphthylphenylbiphenyl diamine) layer is the hole transport layer (HTL) of the TOLED structure and the Alq₃ (Tris-(8-hydroxy-quinoline)aluminum) is the electron transport layer (ETL), which is also the emitting layer (EML). Moreover, the material of cathode is Ag/LiF/Al, which is a popular semi-transparent cathode.²⁰⁻²² The anode is Mo, which has a high work function and a moderate reflectivity (~50%–60%).²⁰ For m-MTDATA, the highest occupied molecular orbital (HOMO) = 5.1 eV, the lowest unoccupied molecular orbital (LUMO) = 2.0 eV, the energy band gap = 3.1 eV, the mobility of electron = $1.0 \times 10^{-3} \text{ cm}^2 \text{ V}^{-1} \text{ s}^{-1}$, and the mobility of hole = $2 \times 10^{-3} \text{ cm}^2 \text{ V}^{-1} \text{ s}^{-1}$. For α -NPD, the highest occupied molecular orbital (HOMO) = 5.6 eV, the lowest unoccupied molecular orbital (LUMO) = 2.5 eV, the energy band gap = 3.1 eV, the mobility of electron = $2.0 \times 10^{-4} \text{ cm}^2 \text{ V}^{-1} \text{ s}^{-1}$, and the mobility of hole = $2 \times 10^{-3} \text{ cm}^2 \text{ V}^{-1} \text{ s}^{-1}$. For Alq₃, the highest occupied molecular orbital (HOMO) = 5.7 eV, the lowest unoccupied molecular orbital (LUMO) = 3.0 eV, the energy band gap = 2.7 eV, the mobility of electron = $2.0 \times 10^{-5} \text{ cm}^2 \text{ V}^{-1} \text{ s}^{-1}$, and the mobility of hole = $1 \times 10^{-5} \text{ cm}^2 \text{ V}^{-1} \text{ s}^{-1}$.²³⁻²⁷ In this paper, we attempt to insert a α -NPD electron blocking layer and change the position of this electron blocking layer to optimize the optical characteristics of the TOLED structure, so that high brightness and highly effective TOLED devices can be obtained. The thickness of the α -NPD electron blocking layer is set to 10 nm. The resonant cavity is designed in such a way that the peak of the standing wave coincides with the electric luminescence (EL) peak of Alq₃. Under this situation, the thickness of HTL must be changed to 10 nm, and the thickness of the α -NPD electron blocking layer must be equal to 10 nm. As indicated in Fig. 1, with the insertion of the α -NPD electron blocking layer, the EML (Alq₃) layer must be divided to two separate parts of thicknesses x nm and $60-x$ nm, respectively.

The absorption and luminescence spectra of Alq₃ are calculated with the APSYS and compared to the experimental results²⁸ as shown in Fig. 2. The Alq₃ emits green light with a peak near 530 nm, and has an absorption spectrum with a peak near 440 nm. Figures 3 (a) and (b) show the current density-voltage ($J-V$) and luminance-current density ($L-J$) characteristics of the TOLED under study. The results obtained from simulations are also in close agreement with those obtained from experiments.

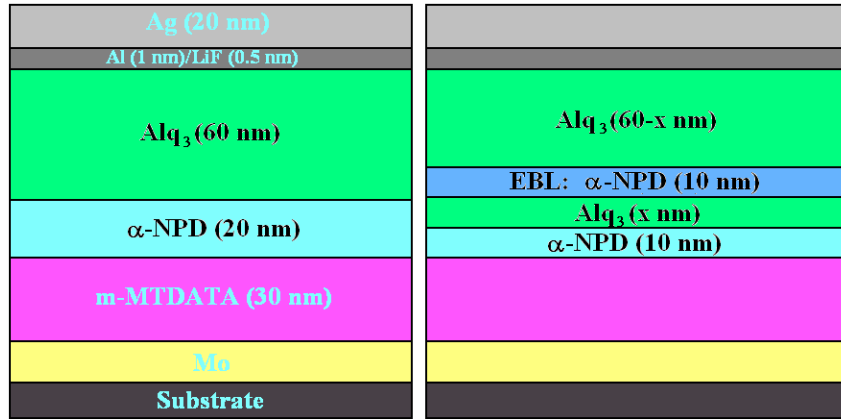


Figure 1. The structures for a typical TOLED (left) and a TOLED with a α -NPD electron blocking layer (right).

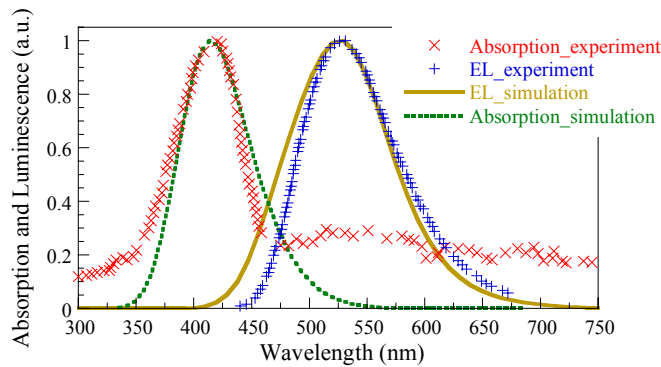


Figure 2. Absorption and emission spectra of Alq₃.

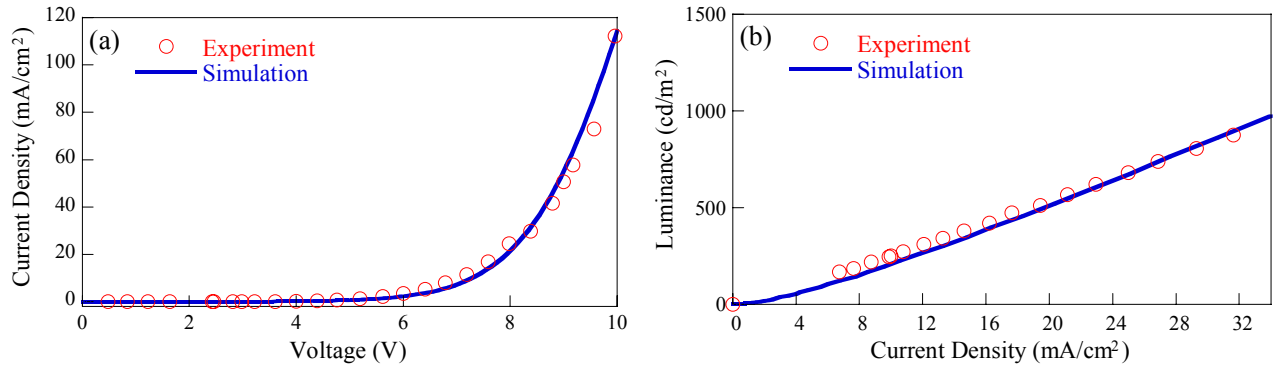


Figure 3. (a) J - V and (b) L - J characteristics of the TOLED device under study.

The typical J - V characteristics of the conventional and proposed TOLEDs are plotted in Fig. 4. It is evident that the J - V characteristics of the proposed devices with a α -NPD electron blocking layer show a much lower current density than the conventional devices at the same driving voltage. However, when the thickness of the EML is equal to 10 nm, the electronic performance of the proposed structure is close to that of the conventional TOLED.

Figure 5 shows the L - J characteristics of the original TOLED device and devices A1 to A5 ($x = 10$ nm to 50 nm, respectively, with a step of 10 nm). The luminance of the original device and A1 to A5 are 1864, 2370, 2358, 2309, 2004, and 1787 cd/m^2 at a current density of 60 mA/cm^2 , respectively. It is obvious that, the proposed TOLED device has good optical performance when the thickness x is 10 nm, while the optical performance is poor when the thickness x is large. Therefore, device A1 has the best electronic and optical performance and is chosen for subsequent studies.

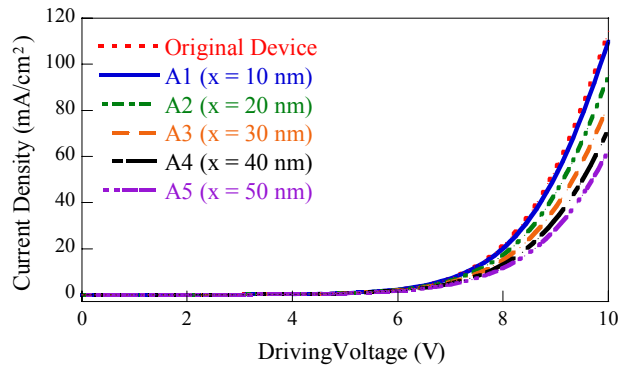


Figure 4. J - V characteristics of original device and A1 to A5.

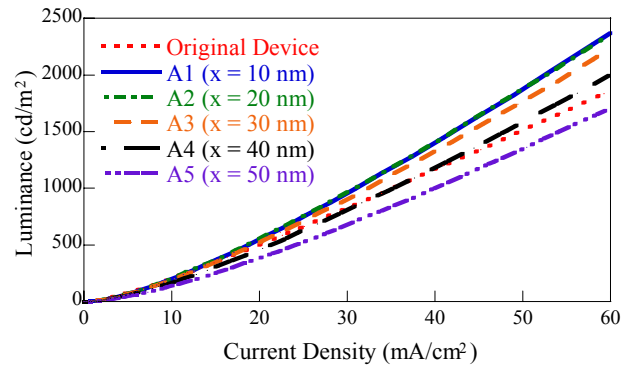


Figure 5. L - J characteristics of original device and A1 to A5.

The energy band diagrams, radiative recombination rates and standing wave distributions of the original device and device A1 are shown in Figs. 6 (a) and (b). The main radiative recombination center of device A1 matches well with the anti-node of the standing wave, but the main radiative recombination center of the original device falls off the anti-node of the standing wave. It is evident that device A1 has stronger micro-cavity effect than the original device. Consequently, device A1 has better optical performance than its original counterpart. Note that, if the position of the α -NPD electron blocking layer is too far away from the anti-node of the standing wave, the optical performance might deteriorate. For examples, as indicated in Fig. 5, the L - J performance of devices A5 and A4 are not as good as that of devices A1 and A2. Moreover, when the value of x is large, the recombination center is near the cathode. In that case, poor optical performance might also be resulted from the fact that the excitons could be quenched by the strong electric field at the cathode.²⁹

From Fig. 6 we notice that there are several recombination centers at the interfaces between adjacent organic layers. These recombination centers could affect the emission spectra of the OLEDs, which in turn result in red shift or blue shift of the peak emission wavelength. As shown in Fig. 6, the radiative recombination rate has a maximum value at the interface of Alq₃ and α -NPD. Device A1 has a larger maximum radiative recombination rate when compared to the original device, while other secondary peaks of radiative recombination rate are smaller than that of the original device. As a result, the radiative recombination rate is increased in device A1, which is presumably due to the fact that the α -NPD has a lower LUMO to block and constrain the electrons in the main recombination region and, hence, more electrons may recombine with holes at the interface of Alq₃ and α -NPD.

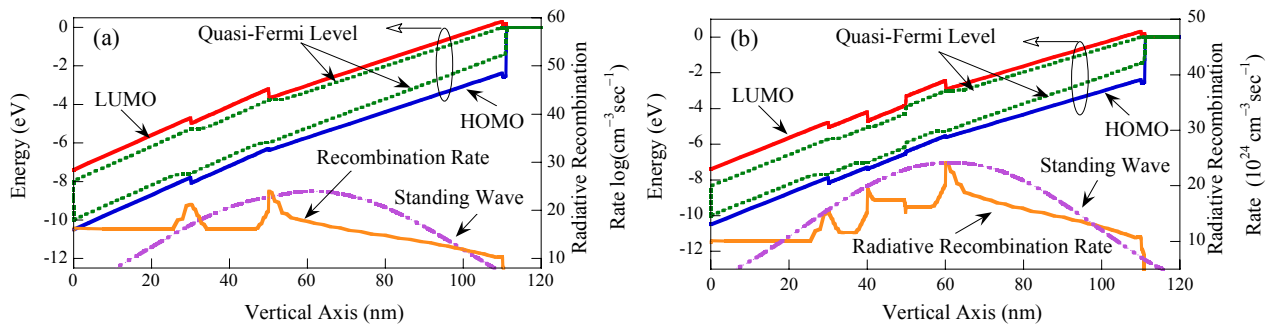


Figure 6. The band diagrams, radiative recombination rates, and standing wave distributions of (a) original device and (b) device A1.

Figures 7 shows the distribution of recombination regions in the TOLED with electron blocking layer (EBL). Regions I, II, and III are the three main recombination regions. The ratio of holes over electrons as a function of thickness x is shown in Fig. 8. We find that the ratio is close to unity in region I of the original device. However, since region I is not the main recombination region, the EL spectrum should be dominated by other recombination regions. From Fig. 8 we find that the numbers of electrons and holes of devices A1 to A5 at region III are more balanced than the original device at region II. Therefore, it is expected that the TOLED device with electron blocking layer will have better optical performance than the original TOLED structure.

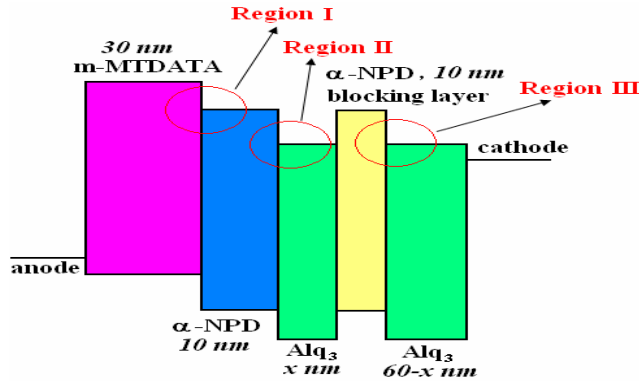


Figure 7. The distributions of recombination regions in the TOLED with EBL.

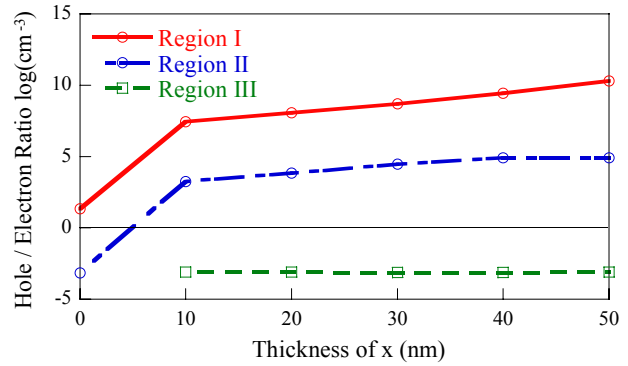


Figure 8. The ratio of holes over electrons as a function of thickness x.

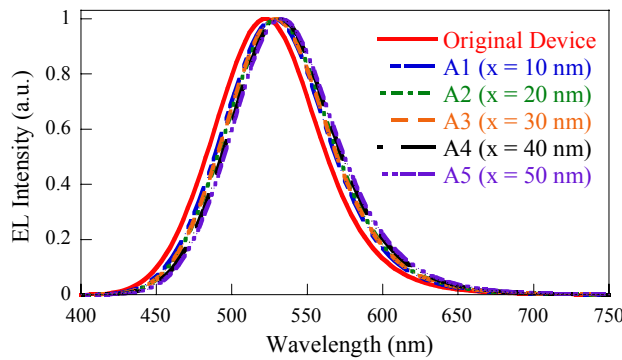


Figure 9. The EL spectra of original device and devices A1 to A5 at 10 volts.

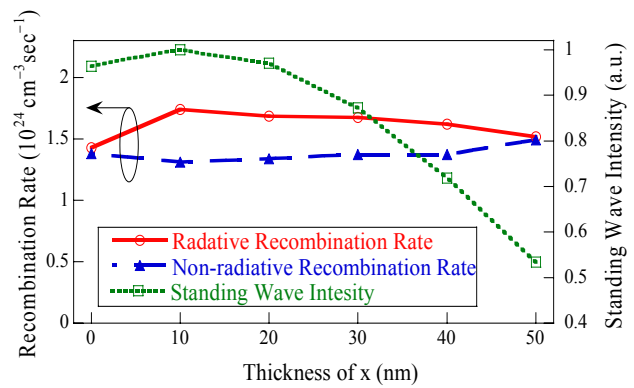


Figure 10. Radiative, non-radiative recombination rate, and wave intensity at different thickness x.

Figure 9 shows the EL spectra of the original device and devices A1 to A5 at 10 volts. It is evident that the peak emission wavelength increases when the thickness x increases, which is due to the overlap of emission spectra created from different recombination regions. Figure 10 shows the radiative recombination rate, non-radiative recombination rate, and standing wave intensity distribution as a function of thickness x. The best performance is obtained when the thickness x is equal to 10 nm, as expected.

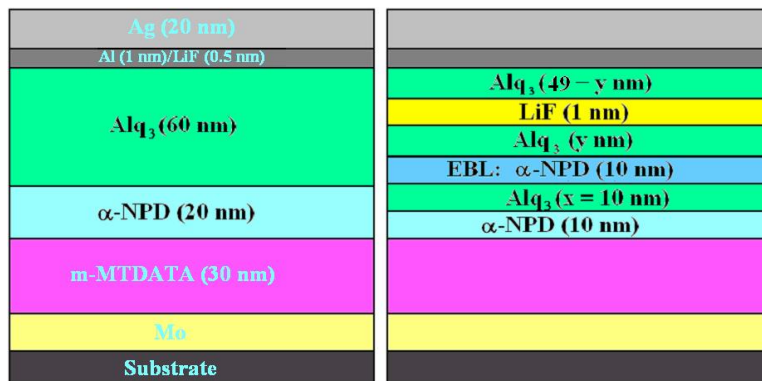


Figure 11. The structures of a typical TOLED (left) and a TOLED with electron and hole blocking layers (right).

From previous study we learn that the optical performance of the TOLED can be markedly improved with the use of a α -NPD electron blocking layer (EBL), as shown in Fig. 1. Now, we wish to verify if the optical performance of the TOLED could be further enhanced with the use of a hole blocking layer (HBL). Indeed, according to the carrier

distribution, there is a need to increase the hole concentration in the main recombination region to improve the carrier balance. Therefore, we tentatively insert a 1-nm-thick LiF layer into the Alq₃ layer to block the holes in an attempt to improve the carrier balance. Considering the situation of standing wave, we must keep the optical thickness of the resonant cavity unchanged. Therefore, we change the total thickness of Alq₃ from 50 to 49 nm because the refractive indices of LiF and Alq₃ are approximately the same ($n \approx 1.7$). Figure 11 shows the TOLED structure with both a 10-nm-thick α -NPD electron blocking layer and a 1-nm-thick LiF hole blocking layer. With the insertion of this 1-nm-thick LiF hole blocking layer, the Alq₃ layer is divided to two separate layers of y nm and $49-y$ nm.

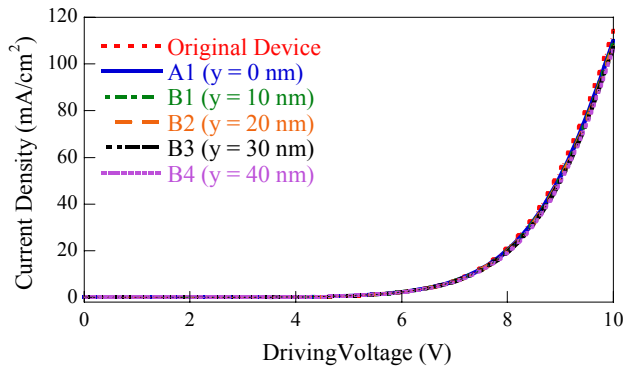


Figure 12. J - V characteristics of original device, A1 and B1 to B4.

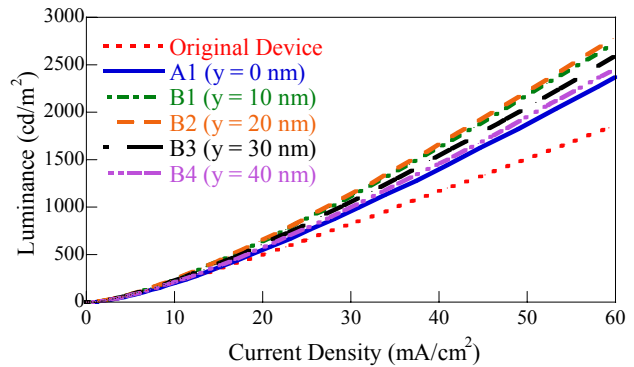


Figure 13. L - J characteristics of original device, A1 and B1 to B4.

The J - V characteristics of the original device, device A1, and devices B1 to B4 are plotted in Fig. 12. Very little difference can be found in these electronic performance curves. The L - J characteristics of the original device, device A1, and devices B1 to B4 are shown in Fig. 13. When the thickness x is 10 or 20 nm, the optical performance of the TOLED devices (B1 and B2) are relatively good. Specifically, the luminance of the original device, A1, and B1 to B4 are 1864, 2370, 3054, 3167, 2925, and 2810 cd/m^2 at a current density of 60 mA/cm^2 , respectively. The EL efficiency of the original device, A1, and B1 to B4 are 3.11, 3.95, 4.55, 4.66, 4.32, and 4.10 cd/A , respectively. Therefore, device B2 has the best optical performance among these devices under study.

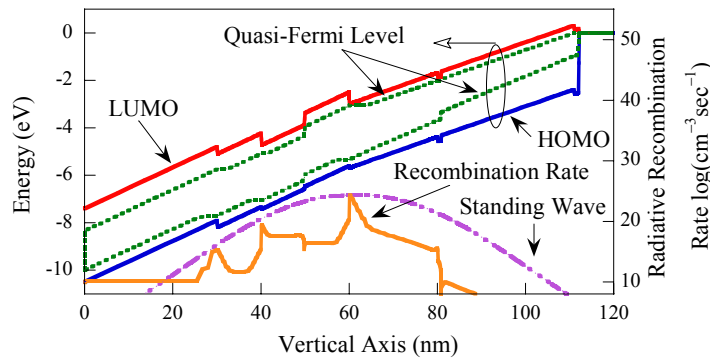


Figure 14. The band diagram, radiative recombination rate, and standing wave distribution of device B2.

The energy band diagram, radiative recombination rate, and standing wave distribution of device B2 are shown in Fig. 14. With the insertion of the LiF layer in the EML, it not only affects the location of the main recombination region but also increases the value of radiative recombination rate. Between the LiF layer and cathode, the quasi-Fermi level is far away from the HOMO of Alq₃, indicating that the concentration of holes will be small in this region. Thus, more holes may be present between the EBL and Alq₃ layer, which is beneficial for improving the carrier balance. Figure 15 shows the hole concentration of the original device, device A1, and devices B1 to B4 near the main recombination region. We find that device B2 has the highest hole concentration. Figure 16 shows the radiative recombination rate, non-radiative recombination rate, and standing wave intensity distribution as a function of thickness y . The best performance is obtained when the thickness y is equal to 20 nm, as expected.

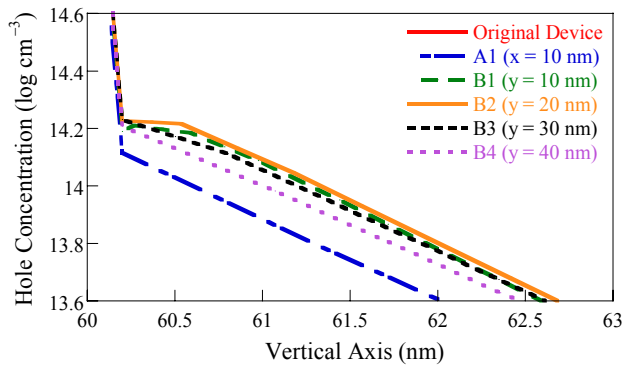


Figure 15. Hole concentration of original device, A1 and B1 to B4.

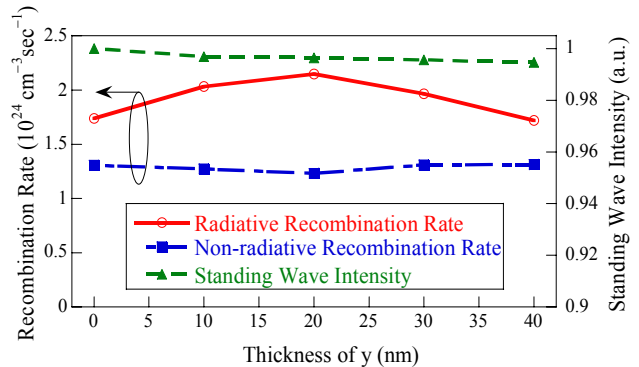


Figure 16. L-J characteristics of original device, A1 and B1 to B4.

4. CONCLUSIONS

Based on a real device fabricated in lab by Yang *et al.*, the electronic and optical properties of top-emitting organic light-emitting diodes (TOLEDs) are investigated with the APSYS simulation program. The simulation results suggest that with the use of both a α -NPD electron blocking layer and a LiF hole blocking layer, the optical performance of the TOLED structure can be improved evidently. Considering the micro-cavity effect, optimization of the TOLED structure under study is attempted.

ACKNOWLEDGMENTS

This work is supported by the National Science Council (NSC) of Taiwan under grant NSC 95-2516-S-018-001-MY3.

REFERENCES

1. C. W. Tang and S. A. VanSlyke, "Organic electroluminescent diodes," *Appl. Phys. Lett.* 51, 913-915 (1987).
2. C. W. Tang, S. A. VanSlyke, and C. H. Chen, "Electroluminescence of doped organic thin films," *J. Appl. Phys.* 65(9), 3610-3616 (1989).
3. A. N. Krasnov, "High-contrast organic light-emitting diodes on flexible substrates," *Appl. Phys. Lett.* 80, 3853-3855 (2002).
4. H. Aziz, Y.-F. Liew, H. M. Grandin, and Z. D. Popovic, "Reduced reflectance cathode for organic light-emitting devices using metalorganic mixtures," *Appl. Phys. Lett.* 83, 186-188 (2003).
5. S. H. Li, H. Liem, C. W. Chen, E. H. Wu, Z. Xu, and Y. Yang, "Stacked metal cathode for high-contrast-ratio polymeric light-emitting devices," *Appl. Phys. Lett.* 86, 143514 (2005).
6. Y. Kijima, N. Asai, N. Kishii, and S.-I. Tamura, "RGB luminescence from passive-matrix organic LED's," *IEEE Tran. Electron Devices* 44, 1222-1228 (1997).
7. Y. Hong, J.-Y. Nahm, and J. Kanicki, "100 dpi 4- α -Si:H TFTs active-matrix organic polymer light-emitting display," *IEEE J. Sele. Top. Quantum Electron.* 10, 16-25 (2004).
8. T. N. Jackson, Y.-Y. Lin, D. J. Gundlach, and H. Klauk, "Organic thin-film transistors for organic light-emitting flat-panel display backplanes," *IEEE J. Sele. Top. Quantum Electron.* 4, 100-104 (1998).
9. J. Kalinowski, L. C. Palilis, W. H. Kim, and Z. H. Kafafic, "Determination of the width of the carrier recombination zone in organic light-emitting diodes," *J. Appl. Phys.* 94, 7764-7767 (2003).
10. Y. M. Kim, J. W. Lee, J. H. Jung, K.-K. Paek, M. Y. Sung, J. K. Kim, and B. K. Ju, "Enhanced brightness and efficiency of organic light-emitting diodes with an LiF in the Alq₃," *IEEE Electron Device Lett.* 27, 558-560 (2006).
11. S. Lee, C.-H. Chung, and S. M. Cho, "Effect of α -NPD film in electron transport layer on electroluminescence color change for organic light emitting devices," *Synthetic Metals* 126, 269-273 (2002).
12. B. Ruhstaller, T. Beierlein, H. Riel, S. Karg, J. C. Scott, and W. Riess, "Simulating electronic and optical processes in multilayer organic light-emitting devices," *IEEE J. Sele. Top. Quantum Electron.* 9, 723-731 (2003).

13. M. Hoffmann and Z. G. Soos, "Optical absorption spectra of the Holstein molecular crystal for weak and intermediate electronic coupling," *Phys Rev. B* 66, 024305 (2002).
14. C. H. Henry, "Theory of spontaneous emission noise in open resonators and its application to lasers and optical amplifiers," *J. Lightwave Tech.* LT-4, 288-297 (1986).
15. APSYS by Crosslight Software Inc., 2005.
16. W. Brutting, S. Berleb, and A. G. Muckl, "Device physics of organic light-emitting diodes based on molecular materials," *Organic Electron.* 2, 1-36 (2001).
17. N. K. Patel, S. Cinà, and J. H. Burroughes, "High-efficiency organic light-emitting diodes," *IEEE J. Sele. Top. Quantum Electron.* 8, 346-361 (2002).
18. P. E. Burrows, Z. Shen, V. Bulovic, D. M. McCarty, S. R. Forrest, J. A. Cronin, and M. E. Thompson, "Relationship between electroluminescence and current transport in organic heterojunction light-emitting devices," *J. Appl. Phys.* 79, 7991-8006 (1996).
19. Vragovi'c, R. Scholz, and M. Schreiber, "Model calculation of the optical properties of 3, 4, 9, 10-perylene-tetracarboxylic-dianhydride (PTCDA) thin films," *Europhysics Lett.* 57, 288-294 (2002).
20. C.-J. Yang, C.-L. Lin, C.-C. Wu, Y.-H. Yeh, C.-C. Cheng, Y.-H. Kuo, and T.-H. Chen, "High-contrast top-emitting organic light-emitting devices for active-matrix displays," *Appl. Phys. Lett.* 87, 143507 (2005).
21. H. Peng, J. Sun, X. Zhu, X. Yu, M. Wong, and H.-S. Kwok, "High-efficiency microcavity top-emitting organic light-emitting diodes using silver anode," *Appl. Phys. Lett.* 88, 073517 (2006).
22. C.-C. Wu, C.-L. Lin, P.-Y. Hsieh, and H.-H. Chiang, "Methodology for optimizing viewing characteristics of top-emitting organic light-emitting devices," *Appl. Phys. Lett.* 84, 3966-3969 (2004).
23. B. Ruhstaller, S. A. Carter, S. Barth, H. Riel, W. Riess, and J. C. Scott, "Transient and steady-state behavior of space charges in multilayer organic light-emitting diodes," *J. Appl. Phys.* 89, 4575-4586 (2001).
24. E. Tutis, M. N. Bussac, B. Masenelli, M. Carrard, and L. Zuppiroli, "Numerical model for organic light-emitting diodes," *J. Appl. Phys.* 89, 430-439 (2001).
25. T. Chasse, C.-I. Wu, I. G. Hill, and A. Kahn, "Band alignment at organic-inorganic semiconductor interfaces: α -NPD and CuPc on InP(110)," *J. Appl. Phys.* 85, 6589-6592 (1999).
26. S. Barth, P. Muller, H. Riel, P. F. Seidler, W. Rieß, H. Vestweber, and H. Bassler, "Electron mobility in tris(8-hydroxy-quinoline)aluminum thin films determined via transient electroluminescence from single- and multilayer organic light-emitting diodes," *J. Appl. Phys.* 89, 3711-3719 (2001).
27. C. Adachi, M. E. Thompson, and S. R. Forrest, "Architectures for efficient electrophosphorescent organic light-emitting devices," *IEEE J. Sele. Top. Quantum Electron.* 8, 372-377 (2002).
28. P. E. Burrows and S. R. Forrest, "Electroluminescence from trap-limited current transport in vacuum deposited organic light emitting devices," *Appl. Phys. Lett.* 64, 2285-2287 (1994).
29. P. Cusumano, F. Buttitta, A. Di Cristofalo, and C. Cal, "Effect of driving method on the degradation of organic light emitting diodes," *Synthetic Metals* 139, 657-661 (2003).